

# Nonlinear evolution of Tayler unstable equilibrium states

D. Elstner<sup>1,\*</sup>, A. Bonanno<sup>1,2</sup>, and G. Rüdiger<sup>1</sup>

<sup>1</sup> Astrophysikalisches Institut Potsdam, An der Sternwarte 16, D-14482 Potsdam, Germany

<sup>2</sup> INAF, Istituto Nazionale di Astrofisica, Osservatorio Astrofisico di Catania, Città Universitaria, Via S. Sofia 78, I-95123 Catania, Italy

Received 2008 Jul 11, accepted 2008 Jul 18

Published online 2008 Aug 30

**Key words** physical data and processes – galaxies – magnetohydrodynamics

We investigate the nonlinear evolution of Tayler unstable toroidal fields in a disk geometry, by numerical simulations. We consider non-rotating and rigid rotating disks, with different radial field profiles. The initial configuration is in equilibrium, which is achieved by a pressure gradient or an external potential force. The nonlinear evolution of the system leads to a stable equilibrium with a current free toroidal field. Only for the fast rotating case we could preserve a ring type structure of the toroidal field.

© 2008 WILEY-VCH Verlag GmbH & Co. KGaA, Weinheim

## 1 Introduction

Recent works by Braithwaite & Spruit (2004), Gilman (2005), Barnes et al. (2004), Kitchatinov & Rüdiger (2008), Arlt et al. (2007), have renewed the interest in the old problem of hydromagnetic stability of stable stratified stellar interiors.

One of the most serious MHD instability which can arise in this case is the current driven (pinch-type) instability of a purely toroidal field because it can proceed via almost horizontal displacements. In fact ever since the paper by Tayler (1973), it has been known that toroidal fields can be unstable close to the axis of symmetry, if there is a non-zero electric current density on the axis. The growth rate of this instability is expected to be of the order of the time taken for an Alfvén wave to travel around the star on a toroidal field line.

Although the inclusion of differential rotation (Rüdiger et al. 2007; Gellert et al. 2008), or of a relatively weak poloidal field (Howard & Gupta 1962; Knobloch 1992; Bonanno & Urpin 2008), alters the stability properties of the system substantially, in physical situations where the Alfvén frequency in the azimuthal direction  $\omega_{a\phi}$  is greater than  $s\nabla\Omega$  which is the inverse characteristic timescale of differential rotation, the Tayler instability will be the dominant one.

The relevant question is then to understand what is the fate of the most unstable mode. For instance, in astrophysical jets, the nonlinear development of the current-driven instability has been analyzed by Lery et al. (2000) who found that this instability can modify the magnetic structure of a jet mainly redistributing the current density in the inner part. Moreover, the numerical simulations of Nakamura et

al. (2006) suggests that the current-driven instability is the dominant instability for the wiggling structures in jets. On the other hand, in the early process of galaxy formation, when the magnetic pressure and the gas pressure are comparable, any large scale radial field could produce an enough strong toroidal field which could then be subject to the Tayler instability.

In this paper we thus investigate the nonlinear evolution of unstable equilibrium solutions in an isothermal disk ring under the presence of a toroidal field. We restrict our investigation to the non-rotating and rigid rotating case. This is a typical configuration which appears in dwarf and irregular galaxies or in the inner part of spiral galaxies.

The structure of the paper is the following: In Sect. 2 we describe the basic elements of the model, and in Sect. 3 we describe the results. Section 3 is devoted to the conclusions.

## 2 The model and basic equations

We consider an isothermal disk ring with a radial extent from  $r_{\text{in}}$  to  $r_{\text{out}}$  and a vertical size of  $h$ . We use dimensionless units normalized with the disk height  $h$ . The time is normalized with 10 sound crossing times  $t_s = 10h/c_s$ . The magnetic field is normalized to the Alfvén speed with the density normalization  $d_0$ . We solve the time dependent ideal MHD equations

$$\frac{\partial \rho}{\partial t} + \nabla \cdot (\rho \mathbf{u}) = 0, \quad (1)$$

$$\frac{\partial \mathbf{u}}{\partial t} + (\mathbf{u} \cdot \nabla) \mathbf{u} = -\frac{\nabla p}{\rho} + \nabla \Psi + \frac{1}{4\pi\rho} [\nabla \times \mathbf{B}] \times \mathbf{B}, \quad (2)$$

$$\frac{\partial \mathbf{B}}{\partial t} = \nabla \times (\mathbf{u} \times \mathbf{B}), \quad (3)$$

\* Corresponding author: delstner@aip.de

$$\nabla \cdot \mathbf{B} = 0, \quad p = c_s^2 \rho, \quad (4)$$

with periodic boundary conditions in  $z$ , reflection in  $r$  and periodic in  $\varphi$ . We use the ZEUSMP2 code in cylindrical coordinates. We varied the number of grid points from  $40 \times 40 \times 40$  up to  $160 \times 160 \times 160$  for some of the models. The results presented in Table 1 are done with the low resolution  $40^3$  and for the models in Table 3 we have chosen  $80^3$  grid points.

First we consider two basic initial equilibrium states with a constant toroidal field. For models with uniform density we introduce an additional potential force in order to have an equilibrium initial state (Model A). In the second case the non-force-free magnetic field is balanced by the pressure gradient of non-uniform radial density distribution (Model B).

For the moment we have no vertical stratification. We apply small random density perturbations to the initial setup and follow the time evolution of the system.

In addition we also consider an initial toroidal field with compact support, defined in a ring inside the computational domain (Model C). In this case we use only the non-uniform density for the initial equilibrium state. Here we also consider rigidly rotating disks, where the centrifugal force is balanced by a fixed gravitational force. All main variables like density, velocity and magnetic field can freely evolve. We have mass and angular momentum conservation for the system. Our boundary conditions give magnetic flux conservation for the field. The  $z$  and  $\varphi$  averaged radial magnetic field has to be zero because of our boundary conditions.

### 3 Results

For a non-rotating disk in ideal MHD Tayler (1973) formulated a necessary and sufficient criterion for stability for the  $m = 1$  modes which, for the cases considered in this paper (no vertical stratification of density and of magnetic field in the basic state) reads

$$g_s \frac{\partial \rho}{\partial s} - \frac{\rho^2 g_s^2}{\gamma P} - \frac{B^2}{s^2} - \frac{2B}{s} \frac{\partial B}{\partial s} > 0. \quad (5)$$

In the case of the ideal Taylor-Couette setup the above condition boils down to  $\frac{d}{ds}(sB_\varphi^2) < 0$  (Rüdiger et al. 2007). That is also the condition for the setup B. For model A one finds for a toroidal field with a radial dependence  $r^q$  stability for  $q = -1$  only. For  $q > -0.5$  the system is always unstable. For  $q < -0.5$  only the region near the axis is unstable. In general we have the condition

$$\frac{B_0^2}{\rho c_s^2} < \frac{-2q - 1}{(1 + q)^2} r^{-2q} \quad (6)$$

for stability.

In our first test we have chosen a constant toroidal magnetic field with  $v_a = 16$ . We found a growth time of 0.15, which is consistent with the inverse of the Alfvén frequency  $\pi r/v_a$  roughly at the inner boundary  $r = 1$ . In Fig. 1 we show a cut of the midplane magnetic field at a time during

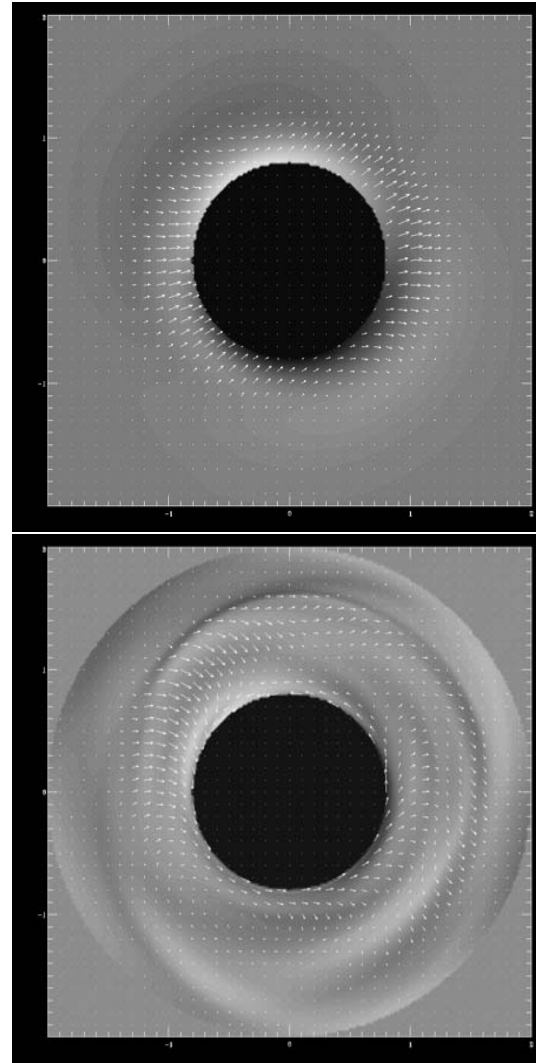


**Fig. 1** Unstable mode for a constant magnetic field (subtracted) during linear growth (*top*) and in the saturated regime (*bottom*).

the exponential growth taken at the maximum radial magnetic energy. We determine the growth time from the maximum growth rate of the radial magnetic energy during the exponential growth phase.

For a fast rigidly rotating system we found no instability if the rotational frequency was larger than the Alfvén frequency. That is consistent with the linear analysis of Pitts & Tayler (1985). If the Lorentz force is compensated by the centrifugal force of the rigid rotation (instead of an additional term in the gravitational potential) the system remains stable, although the situation would change in the case of differential rotation (Rüdiger et al. 2007). Tests with a current free magnetic fields were always stable.

We investigate the nonlinear evolution of the two different initial equilibrium states for a non-rotating isothermal disk with a constant toroidal field. The results are summarized in Table 1. For all models with different field strength or density we found the same value for the normalized growth time  $T_g = t_{\text{growth}} v_a / r_{\text{out}}$ . The fifth and sixth

**Table 1** Models with constant toroidal field.

	Initial Density, $d_0$	$B_0$	$T_g$	$E_k$	$E_m$	$\Delta E_{\text{tor}}$
A0	const, 1	10	1.3	5	6	34
A0A	const, 4	10	1.3	4	4	34
A0B	const, 1	5	1.3	1	1	11
B0	log r, 1	10	1.3	6	6	34

columns denote the maximum kinetic energy  $E_k$ , magnetic energy  $E_m$  during the evolution, excluding the initial energy. The last column gives the difference of the magnetic energy  $\Delta E_{\text{tor}}$  of the toroidal field from the initial state to the final state.

For the models with constant toroidal field we consider a radial range from 0.8 to 2 in normalized length units with the disk thickness.

We define the Alfvén time as  $t_a = r_{\text{out}}/\max(v_a)$ . The non-rotating case is the most unstable configuration. The initial growth is dominated by an azimuthal wave number  $m = 1$  as we checked by a spectral analysis.

During the nonlinear coupling an axisymmetric and higher modes also grow. After  $0.4 t_a$  the magnetic field strength of the radial and vertical component is at the maximum and then decays. A new final equilibrium state is found after  $2 t_a$ . For both cases the toroidal magnetic field is redistributed to a current free state. It means the radial profile is proportional to  $1/r$  that is not the marginal stable solution. From Eq. (5) follows marginal stability for  $r^{-0.5}$  for the models of type B and about  $r^{-0.6}$  for models A for the assumed field strength and sound speed. A simple explanation for the force free solution is the argument that this field has minimum energy for a fixed magnetic flux.

For model A0 we find a radially increasing density, where now the pressure gradient is in equilibrium with the gravitational force initially set to balance the Lorentz force. In model B0 the density is simply redistributed to an uniform one. The unstable modes decay in all cases after the redistribution of the initial constant toroidal field into a current free state.

The magnetic energy is reduced for model A and partly transferred to the potential energy due to the outward transport of matter. The work done by the Lorentz force

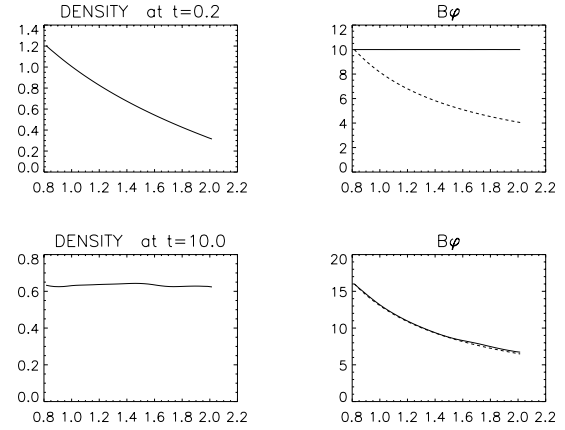
$$\frac{d}{dt} \int_V \frac{B^2}{2\mu} dv = - \int_V \frac{j^2}{\sigma} dv - \int_V \mathbf{u} \cdot (\mathbf{j} \times \mathbf{B}) dv \quad (7)$$

leads also to a reduction of the magnetic energy for model B. Because of the isothermal setup this energy is lost from the system. The maximal (over time) radial rms velocity  $u_r^{\text{rms}} = \text{sqrt} \langle u_r^2 \rangle$  scales with the Alfvén velocity. The radial rms magnetic field strength is proportional to the initial field strength (see Table 2).

During the nonlinear evolution the system develops large scale structures in radial and azimuthal direction. The 1D spectrum in the vertical direction shows a small Kolmogorov range for  $k_z$  approximately between 1 and 10.

**Table 2** rms values for models with constant toroidal field.

Name	$d_0$	$B_0$	$u_r^{\text{rms}}$	$u_z^{\text{rms}}$	$B_r^{\text{rms}}$	$B_z^{\text{rms}}$
A0	1	10	0.4	0.1	1.5	0.4
A0A	4	10	0.2	0.1	1.2	0.4
A0B	1	5	0.2	0.1	0.6	0.2
B0	1	10	2	1	1.3	0.4

**Fig. 2** Radial profiles vertical and azimuthal averaged quantities for initial (top) and final (bottom) state of model B0. The dashed line in the panel of  $B_\phi$  shows the profile  $1/r$ .**Table 3** Models with ring.

	$\Omega$	$d_0$	$B_0$	$T_g$	$\frac{v_{\text{in}}}{v_a^0}$	$E_k$	$E_m$	$\Delta E_{\text{tor}} + \Delta E_{\text{kin}}$
C0	0	5.0	1	0.17	0.1	1.3	0.6	47
C1	0	2.5	1	0.14	0.13	1.5	0.6	47
C2	0	1.25	1	0.12	0.13	1.7	0.6	47
C3	0	2.5	2	0.12	0.1	7	2.5	190
C4	0	2.5	4	0.07	0.1	20	9	772
C5	2	2.5	4	0.08	0	10	5	661+78
C6	1	2.5	4	0.07	0.02	15	9	766+32

Let us now consider an initial toroidal field with compact support (models C), a ring. This is strongly unstable in the inner part of the ring, where the field is a rapidly growing function of the radius. For these set of models we choose  $r_{\text{in}} = 2.4$  and  $r_{\text{out}} = 4.8$ . We define the ring by

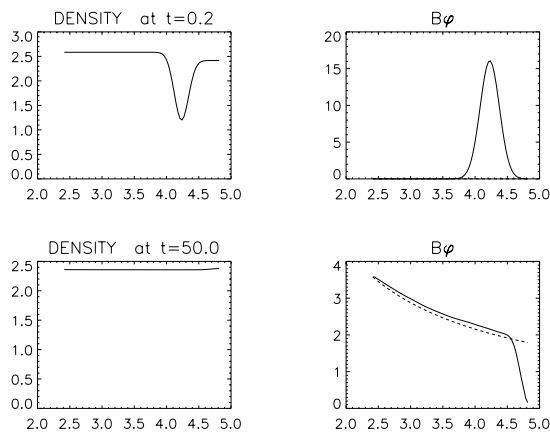
$$B_\phi = B_0 r \exp\left(\frac{(r - r_0)^2}{r_w^2}\right) \quad (8)$$

and set  $r_0 = 4.2$  and the width  $r_w = 0.2$ .

All runs with the ring field are unstable. The growth time is about 0.1 of the Alfvén frequency which is smaller compared to the case of a constant field. There is obviously a dependence on the radial profile of the field, but there is, in addition, a weak dependence of the growth time on the setup. In fact we changed the Alfvén frequency by changing the density (C0–C2) or by field strength (C3–C4). In the second case we also had a greater difference in the magnetic energy between the initial state and the final state, because

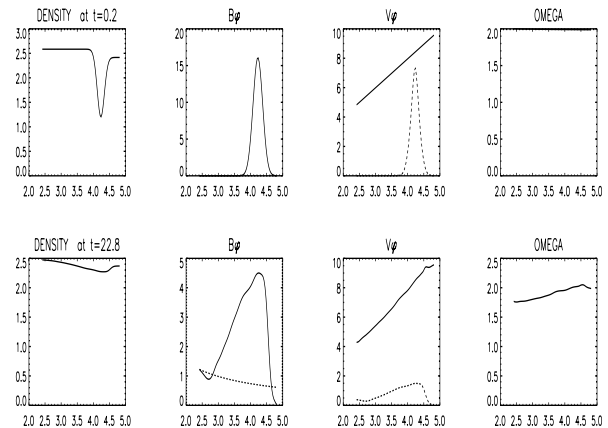
**Table 4** rms values for models with ring field.

Name	$d_0$	$B_0$	$u_r^{\text{rms}}$	$u_z^{\text{rms}}$	$B_r^{\text{rms}}$	$B_z^{\text{rms}}$
C0	5.0	1	0.15	0.01	0.2	0.03
C1	2.5	1	0.23	0.015	0.2	0.03
C2	1.25	1	0.3	0.03	0.2	0.05
C3	2.5	2	0.45	0.05	0.4	0.15
C4	2.5	4	0.9	0.15	0.9	0.3
C5	2.5	4	0.6	0.1	0.8	0.3
C6	2.5	4	0.8	0.15	0.9	0.3

**Fig. 3** Radial profiles vertical and azimuthal averaged quantities for initial (top) and final (bottom) state of model C4. The dashed line in the panel of  $B_\varphi$  shows the profile  $1/r$ .

the absolute value of the initial magnetic energy is different. After the initial exponential growth of the instability the toroidal field moves inward in the nonlinear regime and saturates with an approximately  $1/r$  profile. Only the outer rapidly decreasing part of the field retains its radial shape. In all models we found an inward drift velocity of the field of about one tenth of the initial local Alfvén velocity at the maximum of the ring. We define this velocity  $v_{\text{in}}$  by measuring the time it takes from the initial significant change of the radial profile of  $B_\varphi$  (that is at the end of the exponential growth phase), until the field strength near the inner boundary becomes equal to the maximum field strength at the outer boundary. Because of flux conservation in our setup the maximum field strength decreases.

Model C5 in Table 3 is a fast rigidly rotating disk ring with  $v_\varphi/v_a = 0.5$  (cf. Fig. 4). The maximum of the Alfvén speed is slightly above the rotational velocity at that radius. The growth rate of the instability is surprisingly high nearly the same as in the non-rotating model C4 (cf. Kitchatinov & Rüdiger 2008). The difference appears in the final state, where the maximum of the field is still at the initial radius. Only a broader profile appears. The density is flatter but still has a minimum. As a consequence of angular momentum conservation we see also a change of the rotation into a slower rotation in the inner part, the angular velocity is now slightly growing with increasing radius (cf. Fig. 4). The de-

**Fig. 4** Radial profiles vertical and azimuthal averaged quantities for initial (top) and final (bottom) state of model C5. The dashed line in the panel of  $B_\varphi$  shows the profile  $1/r$ . The dashed line in the panel of the rotational velocity shows half of the Alfvén velocity of the toroidal field.

crease of the maximum Alfvén velocity below the rotational velocity brings the system into an stable equilibrium. For model C6 with half of the rotation rate of model C5 we end up with a similar state as in the non-rotating case. The only difference is the reduced inward drift of the field.

## 4 Conclusion

We investigated the nonlinear evolution of an isothermal disk with a constant toroidal field initially in an stationary equilibrium. The field always relaxes to the current free state without any diffusion only by the action of the Tayler instability. The ring field in an highly conductive system is always unstable, and the field will be transported inwards in a fraction of the Alfvén time. In a rotating system this inward transport time increases until the rotational velocity is of the order of the Alfvén speed and the ring remains stable. This effect could be important for the understanding of the stability of jets and the collimation process. Moreover at the turnover point in the rotation curve of galaxies this type of toroidal field could move inwards quit fast if the Alfvén velocity dominates the rotational velocity. This is probably not the case for grand design spirals, but may be possible in slowly rotating irregulars. The situation may be even more important at higher distance from the midplane, where the rotation becomes weaker.

For the solar tachocline Arlt et al. (2007) presented non-ideal simulations in spherical geometry. They found a rather weak dependence of the instability for the high Reynolds number regime. They extrapolated their results to real solar values and gave an order of 100G for the unstable field configuration. That would mean that the non-ideal solution will not converge to the ideal MHD solution. With a linear stability analysis of the solar tachocline Kitchatinov & Rüdiger (2008) have shown, that non-ideal effects drastically reduce

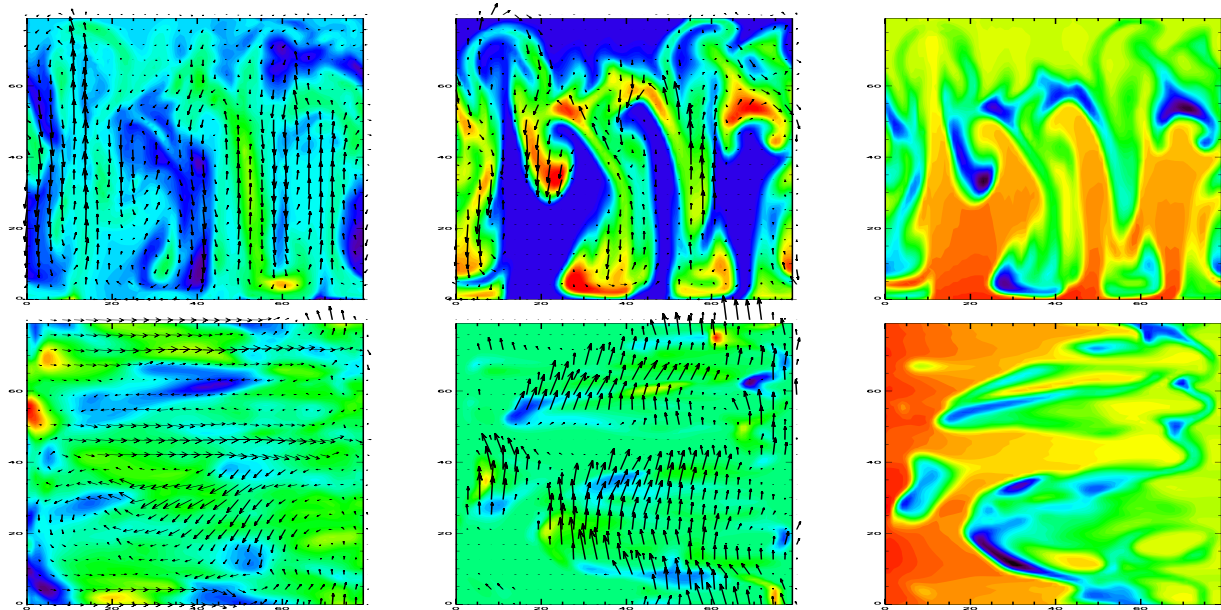


**Fig. 5** Velocity (*left*), magnetic field (*middle*) and density (*right*) of model C2 at time 10. Arrows show the field in the  $z$ - $r$  (*top*) or  $r$ - $\varphi$  plane (*bottom*). The vertical component or the density is color coded. The density is already nearly constant. The variation is about 3%.

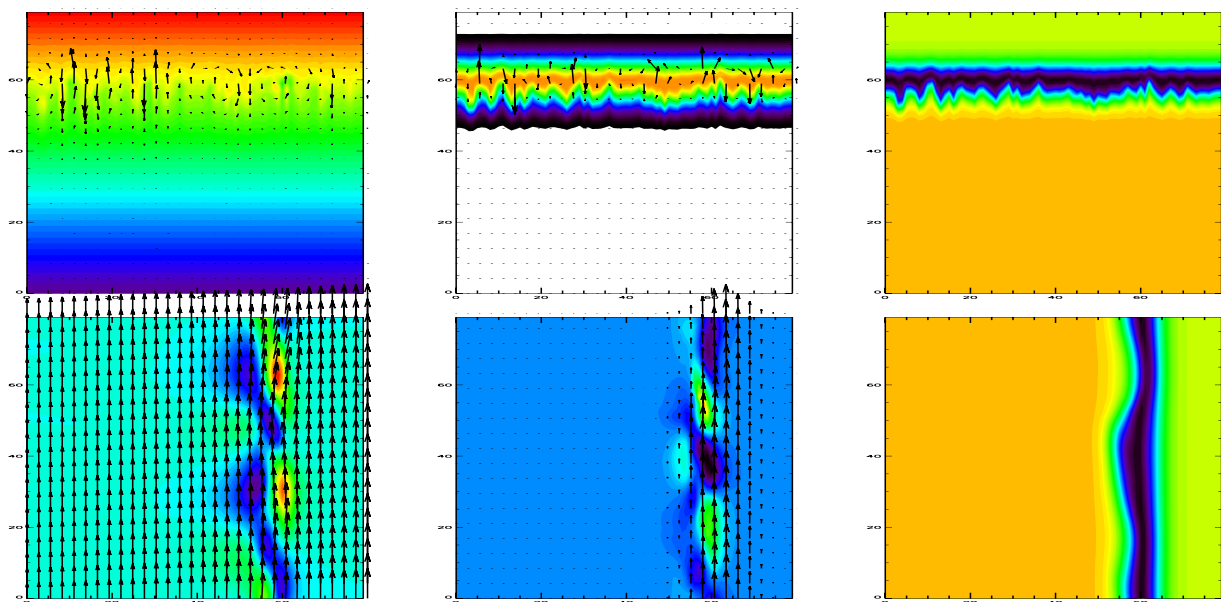


**Fig. 6** Velocity (*left*), magnetic field (*middle*) and density (*right*) of model C6 during the exponential growth phase (time = 0.9). Arrows show the field in the  $z$ - $r$  (*top*) or  $r$ - $\varphi$  plane (*bottom*). The vertical component or the density is color coded.

the critical field strength for the onset of the instability. Nevertheless it would be interesting if the unstable field could be transported into the radiative core. The transport would be rather fast, although the diffusive time scale is small. One can also imagine a turbulent mixing process between radiative core and tachocline.

## References

- Arlt, R., Sule, A., Rüdiger, G.: 2007, A&A 461, 295  
 Barnes, G., Charbonneau, P., MacGregor, K.: 1999, ApJ 511, 466  
 Bonanno, A., Urpin, V.: 2008, A&A 477, 35  
 Braithwaite, J., Spruit, H.: 2004, Nature 431, 819  
 Gellert, M., Rüdiger, G., Elstner, D.: 2008, A&A 479, L33  
 Gilman, P.A., Rempel, M.: 2005, ApJ 630, 615  
 Howard, L., Gupta, A.: 1962, JFM 14, 463  
 Kitchatinov, L.L., Rüdiger, G.: 2008, A&A 478, 1  
 Knobloch, E.: 1992, MNRAS 255, 25  
 Lery, T., Baty, H., Appl, S.: 2000, A&A 355, 1201  
 Nakamura, M., Li, H., Li, S.: 2007, ApJ 656, 721  
 Rüdiger, G., Hollerbach, R., Schultz, M., Elstner, D.: 2007, MNRAS 377, 1481  
 Spruit, H.: 1999, A&A 349, 189  
 Pitts, E., Tayler, R.J.: 1985, MNRAS 216, 139  
 Tayler, R.J.: 1973, MNRAS 161, 365